DOI: 10.1002/ejic.201100820

Proton Sponge Phosphanes: Reversibly Chargeable Ligands for ESI-MS Analysis

Nicola J. Farrer,[a][‡] Krista L. Vikse,[a] Robert McDonald,[b] and J. Scott McIndoe*[a]

Keywords: Proton sponge / Phosphanes / Mass spectrometry / Organocatalysis

Proton sponge phosphanes are unusual ligands in that they possess two basic sites with very different functions: the phosphorus binds to a metal center, while the 1,8-bis(dimethylamino)naphthalene binds protons strongly. Both groups are selective for their target, and the binding of the proton is easily reversible by controlling the pH of the solution. Proton sponge phosphanes therefore make useful chargeable ligands for the purposes of electrospray ionization mass spectrometric analysis of the complexes in which they are bound. However, where the 1,8-bis(dimethylamino)naphthalene is functionalized with the phosphane is critical, and the 1-dimethylamino group can become involved in binding to the metal when diphenylphosphane is in the 2-position. This behavior is undesirable from the point of view of keeping proton and metal binding segregated, and we introduce an efficient synthesis of the 4-substituted proton sponge phosphane in which the two functional groups are on opposite sides of the naphthalene ring. This precaution solves the problem of the molecule acting as a bidentate ligand, but caution is still needed when using the ligand, because ionization pathways such as halide dissociation to form $[M - X]^+$ ions and oxidation of electron-rich metal complexes to form $[M]^{\cdot+}$ can be competitive with protonation.

Introduction

Electrospray ionization mass spectrometry (ESI-MS) has a number of strengths that make it well suited to the study of organometallic catalysis. (1) ESI-MS is a soft technique that operates on solutions and can leave weak bonding interactions intact. (2) Only species that are already charged in solution or contain an easily charged site are detected. Because of this most common solvents are "invisible" and very low detection limits are accessible.[20] (3) Analysis is fast (on the order of seconds), and (4) intermediates at nanomolar concentrations can be detected with ease. Finally, (5) since each species in solution is usually represented by a single peak in the mass spectrum it is often possible to extract information from complex mixtures. A growing body of literature exists in which investigators have taken advantage of these attributes of ESI-MS to study organometallic systems. The first was Berman who used ESI-MS to detect a number of environmentally important organoarsenic ions.[1] Another notable early example comes from Canty in 1993 who reported the positive ESI-MS(/MS) studies of various palladium and platinum organometallic complexes.[2] Since then, a growing application of ESI-MS in this area has been in the identification of short-lived, low-concentration intermediates. It has been used in the study of catalytic oxidation,[3] hydrogenation,[4] hydrosilylation [5] and carbon–carbon bond-forming reactions.[6] A large amount of the attention has been given to palladium-catalyzed carbon–carbon bond-forming reactions.[7] In order to investigate any catalytic system by ESI-MS all species of interest must be charged; either inherently, adventitiously (e.g., by protonation or loss of a halide), or intentionally by installing a charged or chargeable tag.

Monitoring catalytic reactions that have intrinsically or adventitiously charged intermediates is relatively simple, and analyses of these types of systems constitute the bulk of the literature,[8] but many of the most important catalytic organometallic reactions proceed through neutral intermediates where there are no reliable ionization mechanisms for visualization by ESI-MS. In order to study these systems a charged or chargeable (usually having an acidic or basic site) tag is required. Importantly, the tag must not introduce steric or electronic effects that interfere with the catalysis in any way.

In 1994 Canary et al. purposefully used a substrate with an easily protonated site to study the palladium-catalyzed reactions of pyridyl bromide with three different phenylboronic acids by ESI-MS. Pyridyl bromide was selected as a chargeable tag due to the ability of the ring nitrogen to become protonated. Relying on this ionization mechanism, oxidative addition intermediates and transmetallation inter-

[a] Department of Chemistry, University of Victoria,
P. O. Box 3065, Victoria, BC V8W 3V6, Canada
E-mail: mcindoe@uvic.ca
[b] X-ray Crystallography Laboratory, Department of Chemistry, University of Alberta,
Edmonton, AB, T6G 2G2, Canada
[‡] Current address: Department of Chemistry, University of Warwick,
Coventry CV4 7AL, UK

Supporting information for this article is available on the WWW under http://dx.doi.org/10.1002/ejic.201100820.

mediates were observed.[9] Many of the existing studies using charged ligands focus on ruthenium-catalyzed systems, and they often make use of ligands designed to confer water solubility. The groups of Traeger,[10] Nicholson,[11] and Chen[12] have made significant contributions to this area. However, it is still a somewhat under-appreciated approach.

Chargeable tags are neutral molecules that contain a functional group of interest, and at a secondary site bind either an acid or a base to become charged. Chargeable tags (as opposed to permanently charged tags) are appealing for a number of reasons: (i) Any effect that the charged group may have on reactivity is mitigated since the charged tag is in equilibrium with its neutral counterpart, (ii) the pH of the droplet decreases rapidly as the solvent evaporates,[13] so addition of protons is often not required, and (iii) chargeable ligands have the potential to aid in catalyst recovery since their solubility in organic solvents can be manipulated by changing the pH of the reaction mixture.

We have developed chargeable phosphane ligands derived from the strong base 1,8-bis(dimethylamino)naphthalene also known as "Proton Sponge®" that serve as analogues for commonly used organometallic ligands.[14] First studied by Alder and co-workers, Proton Sponge® (**1**) is a very strong, non-nucleophilic base (pK_a = 12.34 in H_2O) with high thermodynamic basicity but relatively low kinetic basicity.[15] **1** binds H^+ by forming intramolecular hydrogen bonds with both nitrogen centers in the molecule to give the charged $[N\cdots H\cdots N]^+$ moiety. **1** has been used extensively as a non-nucleophilic proton abstractor in organic synthesis,[16] and as a matrix material in MALDI-MS.[17]

The high thermodynamic basicity of **1** is attributed to a combination of factors.[18] The methyl groups bound to each nitrogen sterically clash with each other and force the nitrogen lone pairs to point toward each other adopting an "in-in" conformation.[19] This leads to a high degree of lone pair-lone pair repulsion and causes the naphthalene backbone to be twisted. By protonating the neutral molecule a more optimal geometry is attained, steric strain is relieved, and the naphthalene ring returns to planarity.[20] Additional stabilization is gained through the strong intramolecular hydrogen bonds formed between the proton and both nitrogen lone pairs.[18a] The low kinetic basicity of **1** arises from the steric crowding of the basic site by the four nearby methyl groups. These methyl groups and the proximity of the two nitrogen centers to each other are also responsible for the high selectivity that **1** has for H^+; all other cations are too large to fit in the resulting pocket.[21] The overall effect is that **1** is approximately six orders of magnitude more basic than typical aromatic amines, and can selectively trap adventitious protons and become charged.

Results and Discussion

We expected **1** to be a well-behaved electrospray-active tag based on the properties discussed above. Other potentially interfering cations such as Na^+ or K^+ are too large to bind to **1**, so mass spectra of **1** display only the $[M + H]^+$ peak even in the presence of competing cations. Its high ionization efficiency in solution leads to signal intensities approaching those of phosphonium ions allowing for detection at very low concentrations and ensuring that all species containing **1** are represented in the spectrum. Di-protonation is extremely unfavorable and the doubly charged ion is never seen, further simplifying the resulting spectra. Appending **1** to common ligands was anticipated to provide a means of reversibly and selectively charging and investigating a variety of organometallic and coordination compounds and their reactivity. Triphenylphosphane was selected as the parent ligand since it is inexpensive, readily available and is used routinely as a ligand in many catalytic reactions. **1** can be substituted for one of the phenyl groups on phosphorus to give the *ortho*- or *para*-electrospray-active ligands 1,8-bis(dimethylamino)-2-(diphenylphosphanyl)-naphthalene (**3a**) or 1,8-bis(dimethylamino)-4-(diphenylphosphanyl)naphthalene (**3b**) (see Scheme 1).

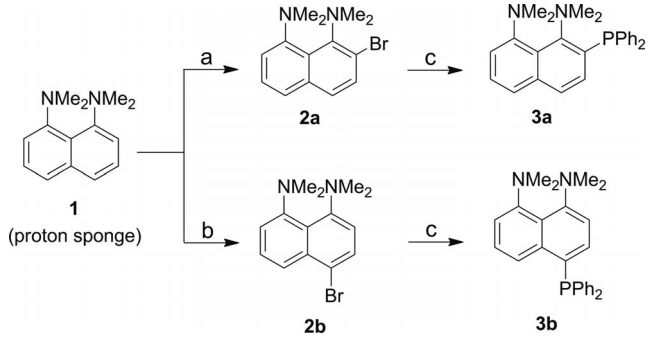

Scheme 1. Synthesis of **3a** and **3b**. a) NBS / THF / –78 °C; 63% yield. b) Br_2 / CCl_4 / 22 °C; 52% yield. c) *n*BuLi / THF / –78 °C, PPh_2Cl / THF / –78 °C.

Initial work on the two isomers revealed that while synthesis of **3a** was straightforward, synthesis of **3b** was not. The problem lies in the first step of the reaction: bromination of **1**, which can be effectively accomplished in the *ortho* (2-) position using the brominating agent *N*-bromosuccinimide, selective for *ortho*-bromination at low temperatures.[22] However, despite attempting the reaction under a variety of brominating conditions that were reported in the literature,[23] selective *para*-bromination at only one of the *para*-sites on Proton Sponge® was elusive. Product mixtures which included *ortho*-substituted and di-substituted compounds were obtained, and purification of **3b** from these mixtures was difficult and low yielding.

3a reacts with a range of metal complexes, including $Fe(CO)_5$, $W(CO)_5$(thf), $PdCl_2$(cod) (cod = cyclooctadiene), and $\{Ru(\eta^6\text{-}p\text{-cymene})Cl_2\}_2$. In the reactions with $Fe(CO)_5$ and $W(CO)_5$(thf), **3a** coordinated only through the phosphorus atom, and the ESI-MS showed only the expected $[M + H]^+$ ions.[14] Reaction of **3a** with $[Ru(\eta^6\text{-}p\text{-cymene})Cl_2]_2$ produced $Ru(\eta^6\text{-}p\text{-cymene})Cl_2$(**3a**) as a crystalline product, but the small orange prisms obtained did not give enough reflections for an X-ray crystallographic structure to be determined. The ESI-MS (in different solvents, in-

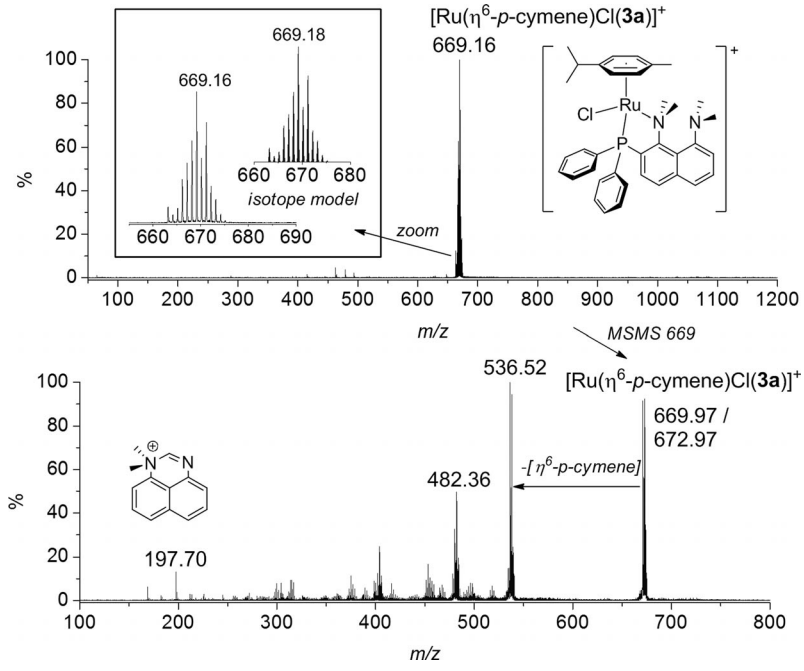

Figure 1. Positive-ion ESI-MS and MS/MS of [Ru(η^6-*p*-cymene)Cl(**3a**)]$^+$ in CH_2Cl_2. Fragmentation by loss of *p*-cymene rather than loss of **3a** is strong evidence that **3a** is strongly bound and hence not monodentate.

cluding CH_2Cl_2, MeOH, and MeCN) suggested that a chloride ligand had been displaced, as the product appeared to be [Ru(η^6-*p*-cymene)Cl(**3a**)]$^+$ rather than [Ru(η^6-*p*-cymene)Cl_2(**3a**) + H]$^+$. Assessment of NOE interactions (2D ^{1}H NOESY) allowed assignment of the ^{1}H NMR spectrum (see Supporting Information Figure SI2) to give the structure shown in Figure 1. The bulky proton sponge group is seen under the methyl end of the *p*-cymene, rather than the isopropyl end, which is attributed to steric interactions. The protons on the dimethylamino groups nearest to the ruthenium center are deshielded (4.18, 4.02 ppm) and chemically distinct from each other [by way of comparison, in the Fe complex $Fe(CO)_4$(**3a**) the same protons are seen as one signal at δ = 2.41 ppm], indicative of a substantial nitrogen lone pair interaction with the ruthenium.

Evidently the proton sponge functionality was coordinating to the metal in this case and so further complexes were investigated to determine the generality of this behavior. Reaction of $PdCl_2$(cod) with **3a** produced $PdCl_2$(**3a**)$_2$ through displacement of the weakly bound cod ligand by two equivalents of **3a**, and an X-ray crystal structure determination was carried out (Figure 2, CCDC-837948).

The structure shows an essentially conventional triarylphosphane ligand, with some distortion due to the bulk of the proton sponge in the *ortho* position. The considerable bulk of **3a** is evident from the structure, so it is therefore not surprising that the *trans* isomer is favored. The phosphane ligand in *trans*-$PdCl_2$(**3a**)$_2$ is calculated to have a cone angle[24] of 169° with measurements taken directly from the crystal structure. The cone angle of PPh_3 in the triphenylphosphane analogue *trans*-$PdCl_2(PPh_3)_2$ is 146° when calculated by the same method.[25]

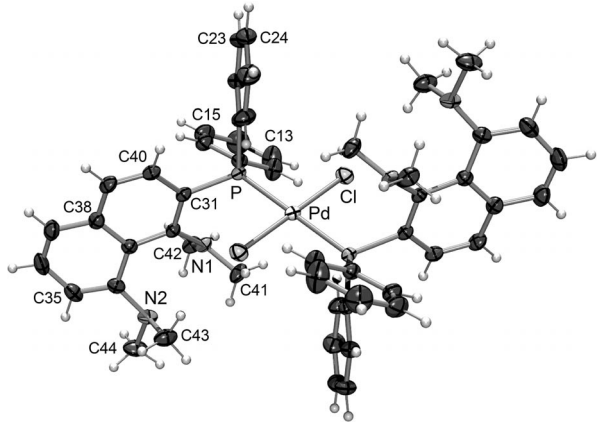

Figure 2. Single-crystal X-ray structure of *trans*-$PdCl_2$(**3a**)$_2$. Key bond lengths: Pd–Cl 2.312 Å; Pd–Cl 2.349 Å; P–C31 1.824 Å; C42–N1 1.427 Å; Me–N (1.45 ± 0.015) Å. Key bond angles: P–Pd–Cl (90 ± 1)°, Pd–P–C31 113.99°, Pd–P–C21 103.12°, Pd–P–C31 125.87°. Key torsion angle: N1–C42–C34–N2 9.00°.

ESI-MS of *trans*-$PdCl_2$(**3a**)$_2$ in CH_2Cl_2 or MeOH gave no discernible signal, but mixtures of the solvents or addition of a small amount of formic acid enabled detection of charged derivatives of the complex (Figure 3). Free ligand [**3a** + H]$^+$ at *m*/*z* 399.06 was the most intense signal, less intense (palladium) species were seen at higher values. The parent complex $PdCl_2$(**3a**)$_2$ ionized principally through two different pathways: loss of Cl^- gave [PdCl(**3a**)$_2$]$^+$ at *m*/*z* 938.91 whereas addition of H^+ gave [$PdCl_2$(**3a**)$_2$ + H]$^+$ at *m*/*z* 974.89.[26] In the presence of formic acid, the intensity of these two peaks was approximately equal despite the large excess of acid available. In CH_2Cl_2/MeOH with no

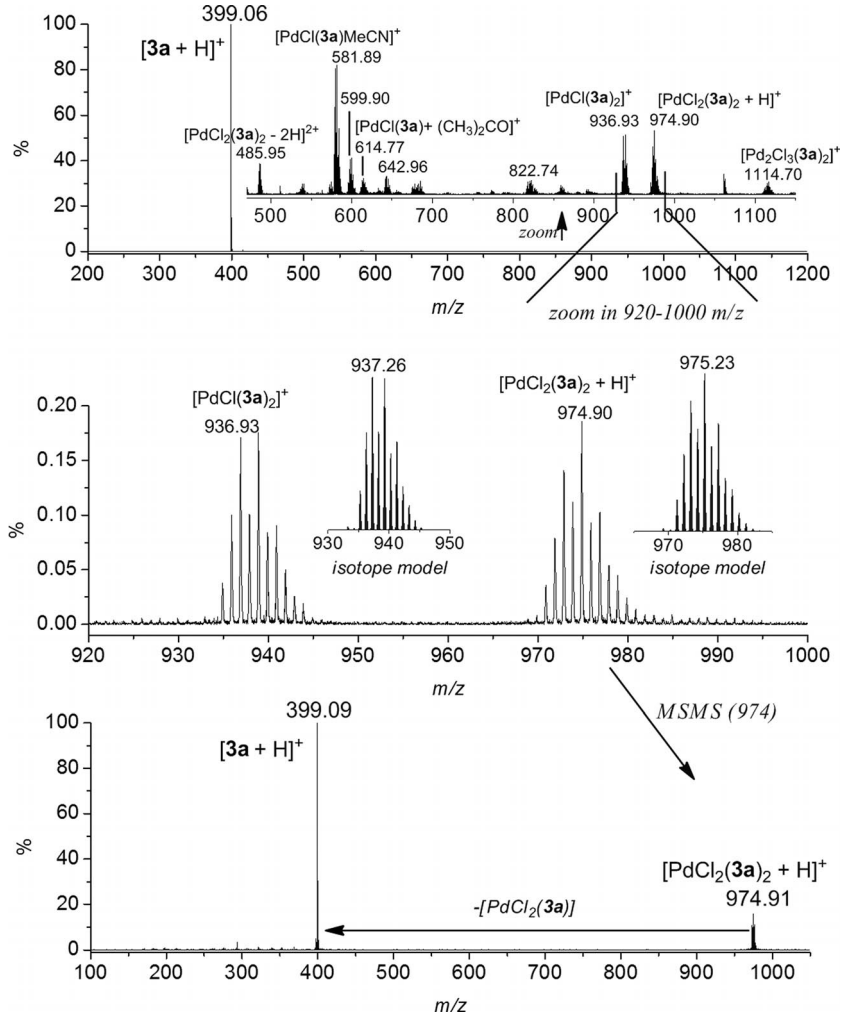

Figure 3. Top: ESI-MS (CH_2Cl_2/formic acid) of $PdCl_2$(**3a**)$_2$. Middle: enlargement of *m*/*z* 920–1000 region. Bottom: MS/MS of [$PdCl_2$(**3a**)$_2$ + H]$^+$. MS/MS of the species at *m*/*z* 485.95 and *m*/*z* 581.89 are shown in the Supporting Information.

added acid the loss of Cl^- was dominant. The intensity of the palladium species in the presence of acid was much lower than in CH_2Cl_2/MeOH, as the acid causes some decomposition of the original complex to generate a small quantity of free ligand [**3a** + H]$^+$. [PdCl(**3a**)$_2$]$^+$ showed a strong affinity for CH_3CN despite only trace amounts being present in the mass spectrometer; [PdCl(**3a**)(CH_3CN)]$^+$ is seen at *m*/*z* 581.89, and the unsolvated complex [PdCl(**3a**)]$^+$ is seen at a lower intensity at *m*/*z* 538.90. Fragmentation of [PdCl(**3a**)(CH_3CN)]$^+$ showed facile loss of the CH_3CN at low collision energies (Supporting Information, Figure SI2). The acetone adduct [PdCl(**3a**)(Me_2CO)]$^+$ was detected at *m*/*z* 614.77. The complexity of the palladium speciation led us to synthesize the platinum equivalent, $PtCl_2$(**3a**)$_2$, which did ionize predominantly by addition of a proton rather than by chloride loss (see Supporting Information, Figure SI3), though the high abundance of free [**3a** + H]$^+$ confirmed that **3a** was rather labile.

The propensity of the ligand to ionize through chloride displacement was troubling, because ideally the chargeable group should provide a unique ionization pathway that does not involve alteration of the coordination sphere of the metal. We therefore examined a palladium complex that did not contain chloride, namely Pd(dba)$_2$ (dba = dibenzylideneacetone), which is a useful precursor to Pd^0 phosphane complexes, as the dba ligands are easily displaced. Unfortunately, complicated reactivity ensued and no species of the form [Pd(**3a**)$_n$ + H]$^+$ (*n* = 1, 2, 3) were detected. Instead, the Pd^0 appeared to activate the proton sponge functional group and species of the form [**1** – H]$^+$ were detected, suggesting the ligand had undergone C–P bond activation. The final nail in the coffin for **3a** was that it did *not* promote cross-coupling reactions, including simple Suzuki and Sonogashira couplings that worked well with triphenylphosphane. **3a** was therefore abandoned as a useful ligand, as the proximity of the proton sponge functionality to the metal center compromised the reactivity we hoped to study: it failed the test of a useful chargeable tag for ESI-MS studies.

This nonideal reactivity caused us to revisit **1**, substituted in the *para* position as a charged ligand with the aim of inhibiting unwanted participation of the proton sponge functionality in reactions since the chargeable dimethylamino groups of **3b** are further removed than those of **3a**

and are unable to interfere with reactivity at the metal center. A synthesis was developed under which **3b** could be produced with an overall isolated yield of 19% in two steps (Scheme 1). **2b** was synthesized by dropwise addition of bromine (diluted in carbon tetrachloride) to a carbon tetrachloride solution of **1** at room temperature. This addition must be performed slowly (ca. 2.5 h) to maintain selectivity for **3b**. After addition of aqueous solutions of sodium thiosulfate and sodium hydroxide, ESI-MS showed good selectivity for addition of only one bromine atom to **1** (only small amounts of **1** at *m*/*z* 215, and the di-brominated side product, *m*/*z* 457, are observed); although MS could not distinguish between *ortho*- and *para*-brominated isomers (Supporting Information, Figure SI4). After workup, ^{1}H NMR confirmed that the correct isomer was formed (Supporting Information, Figure SI5) in a ratio of 93:7 (*para*:*ortho*), the reverse of the ratio obtained in the synthesis of **2a** when NBS at –78 °C is used for bromination (9:91). **2b** was used without further purification to form **3b** via lithiation and treatment with PPh_2Cl at low temperature in THF. The mixture was warmed to room temperature with stirring and then allowed to settle. After filtration, deep orange crystals of **3b** were formed in the filtrate via solvent evaporation. An X-ray crystal structure determination was performed on a single crystal of **3b** (Figure 4, CCDC-837947).

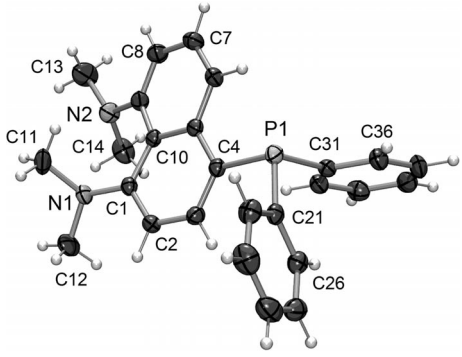

Figure 4. Single-crystal X-ray structure of **3b**. Key bond lengths: P1–C (1.838 ± 0.002) Å; C1–N1 1.402 Å; C9–N2 1.404 Å; N–C_{Me} (1.452 ± 0.002) Å. Key bond angles: C21–P1–C31 101.98°; C21–P1–C4 100.94°; C31–P1–C4 102.28°. Key torsion angle: N1–C1–C9–N2 22.75°.

Comparison of the structure of **3b** to that of **3a**[14] reveals that the torsion angle reflecting the in-and-out of plane bending of the dimethylamino groups is 22.8° in **3b**, significantly less than the 37.4° seen for **3a**. The reduced strain is no doubt due to the –PPh_2 group being moved from the proximal 2- to the remote 4-position. The N···N distance is correspondingly reduced, from 2.90 to 2.78 Å. Like **3a**, **3b** displays pH-dependent water solubility[27] – the unprotonated form is soluble in organic solvents only, addition of acid protonates the sponge functionality and allows aqueous dissolution.

The mass spectrum of **3b** gave the expected single, intense $[M + H]^+$ peak (Figure 5). To test the behavior of the tag when coordinated to a metal center, a solution of $PdCl_2$(cod) in dichloromethane was combined with a solution of **3b** in dichloromethane and an ESI-MS of the mixture was collected. The major signal in the spectrum (*m*/*z* 975) corresponds to $[PdCl_2(\mathbf{3b})_2 + H]^+$ in which one of the chargeable ligands is protonated. In contrast to **3a**, no signal corresponding to ionization by loss of chloride (*m*/*z* 940) was observed, and very little of the free ligand is observed (*m*/*z* 399) suggesting that **3b** performs well as a ligand for palladium.

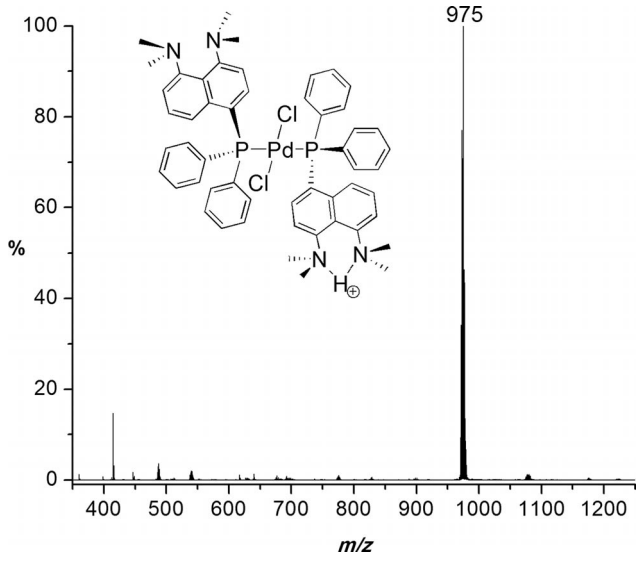

Figure 5. Positive-ion ESI-MS of a dichloromethane solution of $PdCl_2$(cod) and **3b**. Small peaks are observed at: *m*/*z* 415 for the oxidized ligand $[\mathbf{3b}O + H]^+$, *m*/*z* 488 for the doubly charged complex $[PdCl_2(\mathbf{3b})_2 + 2H]^{2+}$, and *m*/*z* 539 and *m*/*z* 1077 for the singly and doubly protonated versions of the dimer $Pd_2Cl_2(\mathbf{3b})_2$, respectively.

Given the success of **3b** as a chargeable tag, we next employed **3b** in the study of a catalytic reaction. Our goal was to study palladium-catalyzed systems, and to that end we chose a Stille reaction, which Santos had previously studied by ESI-MS,[28] to test the performance of our chargeable ligand. An acetonitrile solution containing the catalyst $Pd(OAc)_2$ and **3b** was examined by MS, and the result was somewhat disappointing (Figure 6). While species consistent with the ones reported by Santos were detected, more than one ionization pathway was operative; protonation of **3b** was observed, and many of the palladium-containing species were also oxidized to form radical cations. The latter ionization method involves oxidation of Pd^0 at the tip of the electrospray capillary – the very method that Santos relied on in his experiments to obtain positive ions. We had anticipated that protonation of **3b** would be correspondingly more facile, suppressing oxidation of palladium. However, this was not the case.

Why do the radical cations form? ESI-MS owes much of its sensitivity to the creation of an excess of positive (or negative, depending on the ionization mode) charge on the droplets. It does so through electrochemistry – a tiny amount of material is oxidized at the capillary. Typically,

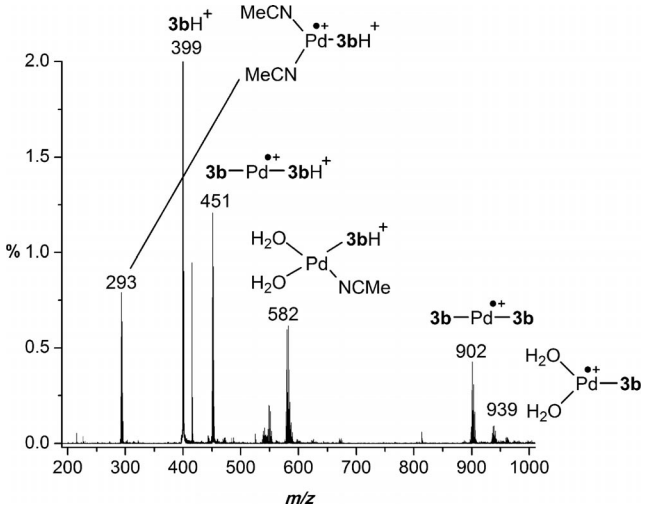

Figure 6. Positive-ion ESI-MS of an acetonitrile solution of $Pd(OAc)_2$ and **3b**.

this process is invisible because the oxidized material, often the iron in the stainless steel capillary, rarely appears in the mass spectrum (its surface activity is low). However, Pd^0 phosphane complexes are both greasy (hydrophobic, surface active) and very easily oxidized, more so than the capillary.

Further investigation of the Stille reaction using **3b** produced spectra containing many peaks that were difficult to assign (Supporting Information, Figure SI6). We attributed these peaks to the products of unknown reactivity involving the radical species formed in the electrospray ionization process and we conclude that while **3b** can perform as an ESI tag, it is not suited to the study of systems for which there are efficient alternative metal-based ionization pathways. It should be noted, however, that Pd^0 is an unusually challenging system, and that for less electron-rich metal complexes, the idea remains valid.

The difficulty in obtaining interpretable MS data on palladium-catalyzed reactions using chargeable ESI tags led us to the investigation of permanently charged ESI tags for the study of these systems.[29] Permanently charged ESI tags have the advantage of (1) being less pH-dependent than chargeable tags, and (2) having fewer potential avenues for reactivity that may interfere with the system of interest. In our experience, the use of a permanently charged tag generally results in simpler spectra.[30] Ammonium or phosphonium groups are most commonly employed as the charged group,[31] and if solubility of the molecule in organic solvents is compromised due to the addition of this polar group, the counterion may be exchanged to obtain more desirable solubility properties.

Conclusions

Proton sponge derivatized phosphane ligands possess – theoretically at least – many of the properties desirable for a chargeable ESI-MS tag. Alone, they are selective for ionization by protons, even in the presence of other cations. Their ionization efficiency is good. They coordinate readily to metal complexes through the phosphorus. However, they have weaknesses that hamper their ability to perform reliably: their ionization is dependent on the acidity of the solution, they are bulkier than the parent triphenylphosphane (especially for **3a**, the *ortho*-substituted sponge), coordination by the sponge functionality can be problematic, and reactivity can be substantially different to the parent triphenylphosphane.

Experimental Section

General: Dry solvents were obtained from an MBraun solvent purification system. All solvents were HPLC grade unless otherwise stated. Reagents were purchased from Aldrich and used without further purification except for **1**, which was recrystallized from hot methanol. Reactions performed under nitrogen were carried out using standard Schlenk techniques. All electrospray ionization mass spectra were collected with a Miromass Q-TOF *micro* instrument. Capillary voltage was set to 2900 V, source temperature was 80 °C and desolvation temperature was 150 °C. Samples were infused via syringe pump at 10 μL min^{-1}. NMR spectra were recorded with a Bruker AC-300 spectrometer. Chemical shifts are quoted in ppm using internal references of $CDCl_3$ (^{1}H δ = 7.26 ppm) or CD_3CN (^{1}H δ = 1.94 ppm) where appropriate. Melting points were recorded with a Gallenkamp melting point apparatus and are uncorrected. IR spectra were recorded using a solution cell in a Perkin–Elmer Spectrum 1000 FT-IR spectrometer.

[1,8-Bis(dimethylamino)naphthalene-4-yl] Bromide (2b): A solution of bromine (2.15 mL, 41.7 mmol) in carbon tetrachloride (40 mL) was added dropwise over 2.5 h to a stirring solution of **1** (10.0 g, 46.6 mmol) in carbon tetrachloride (60 mL) under an inert atmosphere, resulting in a dark red solution. To this, aqueous solutions of sodium thiosulfate (1 M, 20 mL) and sodium hydroxide (20% w/v, 20 mL) were added dropwise with stirring. The resultant yellow-brown mixture was filtered and the beige byproduct was washed (CH_2Cl_2). The organic layer was collected and the volume reduced to give **2b** as a red-brown oil (7.07 g, 52% crude yield). The product was used directly without further purification to synthesize **3b**. ^{1}H NMR (300 MHz, $CDCl_3$): δ_H = 7.80–6.71 (m, 5 H, aromatic protons), 2.81–2.77 [m, 12 H, 2(N*Me*$_2$)] ppm.

[1,8-Bis(dimethylamino)naphthalene-4-yl]diphenylphosphane (3b): A solution of **2b** (1.5 g, 5.1 mmol) in THF (15 mL) was cooled to –78 °C and *n*BuLi (3.3 mL, 1.6 M in hexanes, 5.1 mmol) was added dropwise with stirring, after which the solution was stirred for a further 30 min resulting in an amber-colored solution. Chloro-diphenylphosphane (1 mL, 5.4 mmol) was added dropwise with vigorous stirring, and stirring was continued (–78 °C, 2 h) giving a red-orange solution. The mixture was warmed to room temperature and the yellow-brown precipitate isolated by filtration. Orange crystals of **3b** were collected from the filtrate by solvent evaporation (37% yield). ^{1}H NMR (300 MHz, $CDCl_3$): δ_H = 7.98 (m, 1 H, naphthalene proton), 7.27 (m, 11 H, phenyl protons and one naphthalene proton), 6.90 (d, 1 H, naphthalene proton), 6.78 (m, 2 H, naphthalene proton), 2.804 [s, 6 H, N(C*H*$_3$)], 2.799 [s, 6 H, N(C*H*$_3$)] ppm. ^{31}P NMR (360 MHz, $CDCl_3$): δ_P = –13.41 [s, *P*Ph$_2$($C_{10}H_{17}N_2$)] ppm. M.p. 168–169 °C.

Reaction of [Ru(η^6-*p*-cymene)Cl$_2$]$_2$ with 3a in MeOH: Adapted from ref.[32] A methanolic solution of **3a** (2 equiv., 0.131 g, 0.33 mmol)

and [Ru(*p*-cymene)Cl_2]$_2$ (0.101 g, 0.165 mmol) was refluxed for 3 h with monitoring (ESI-MS), after which time the reaction was judged to be complete (absence of free **3a**). The solution was left to stand for 2 d, reduced in volume and layered with pentane. Crystallizations were set up, eventually the product decomposed to black oil. ESI-MS (after 2 h reflux, MeOH, selected peaks): *m*/*z* (%) = 634.94 (40) [Ru(η^6-*p*-cymene)(**3a**) + H]$^+$, isotope model (635.22), 874.53 (3) [Ru_2(η^6-*p*-cymene)(MeOH)Cl_3(**3a**)]$^+$, isotope model (875.05). MS/MS (635) [Ru(η^6-*p*-cymene)(**3a**) + H]$^+$): *m*/*z* (%) = 496.41, 457.35, 379.10, 298.81 (major Ru species) and 197.70 ([**M** – CH_4]$^+$, model 198.11). MS/MS (874), [Ru_2Cl_3(η^6-*p*-cymene)(**3a**)MeOH]$^+$: *m*/*z* (%) = 872.56, general Ru "grass" between 800 and 400, 213.8 ([**M** – H]$^+$, model 213.14).

Reaction of [Ru(*p*-cymene)Cl_2]$_2$ with 3a in MeCN/toluene: The compounds **3a** (13 mg, 0.033 mmol) and [Ru(*p*-cymene)Cl_2]$_2$ (10 mg, 0.017 mmol) were placed in a flask, which was evacuated and placed under N_2. CD_3CN (1 mL) was added, the solution mixed and filtered into an NMR tube. The reaction was monitored by ^{31}P and ^1H NMR at regular intervals. ^{31}P NMR yield 80%. ^1H NMR (360 MHz, CD_3CN, [Ru(η^6-*p*-cymene)Cl_2]$_2$): δ_H = 5.54 (d, *J* = 6.1 Hz, 4 H, Ar*i*Pr), 5.29 (d, *J* = 6.2 Hz, 4 H, Ar_{Me}), 2.90 (septet, *J* = 7.0 Hz, 2 H, Hi_{Pr}), 2.22 (s, 6 H, Me), 1.29 [d, *J* = 7.0 Hz, 12 H, 2(*i*Pr)Me] ppm. ^{13}C NMR {90 MHz, CD_3CN, [Ru(η^6-*p*-cymene)Cl_2]$_2$}: δ_C = 103.52 (quat, Ar_{iPr}), 99.99 (quat, Ar_{Me}), 84.63 (Ar_{Me}), 82.21 (Ar_{iPr}), 31.79 (secondary *i*Pr), 22.38 (*i*PrMe), 18.96 (Me) ppm. Main product, [Ru(*p*-cymene)(Cl)(**3a**)][Cl]. ^{31}P NMR (red crystals, 146 MHz, CD_3CN): δ = 52.69 (s) ppm. ^1H NMR (360 MHz, CD_3CN): δ_H = 7.85 [ddd, *J* = 11.3, 1.1, 8.3 Hz, 2 H, H_{12}, NOE to *p*-cymene (5.07)], 7.71–7.49 (m, 12 H, 1 5-H, 1 4-H, 2 12′-H, 2 13-H & 2 13′-H, 1 14-H & 1 14′-H, 6-H, 7-H) ppm. Within this: 7.54–7.58 (4-H), 7.28–7.16 (m, impurity, 2 H), 7.12 (dd, 1 H, *J* = 8.4, 9.6 Hz, coupling to ^{31}P, H^3), 6.28 (dd, *J* = 7, 1 Hz, 1 H, *p*-cymene ring, NOE to *i*Pr group at 1.22 and 6.07), 6.25 (dd, *J* = 5.2, 1 Hz, 1 H, *p*-cymene ring, NOE to 5.07 and Me at 1.53), 6.07 (dd, *J* = 6.3, 1 Hz, 1 H, *p*-cymene ring, NOE to Me group at 4.02 and Me group at 1.53), 5.07 (dd, *J* = 6.0, 1.5 Hz, 1 H, *p*-cymene ring, NOE to *i*Pr CH group and 6.25, NOE to H_{12} at 7.85), 4.18 [d, *J* = 0.5 Hz, 3 H, NMe group, on C_{1back}, NOE to 6.07 (weak) *and* 6.25 *p*-cymene proton], 4.02 (s, 3 H, Me, NMe group, on C_{1front}, NOE to 6.07 *p*-cymene, NOE to *p*-cymene Me at 1.53), 2.90 (s, 3 H, NMe group on $C8_{back}$, NOE to NMe at 4.18 and weak NOE to NMe at 4.02), 2.78 (septet, *J* = 6.9 Hz, 1 H, *i*Pr CH, NOE to both 1.22 and 1.18, and 5.07), 2.27 (s, NMe group on $C8_{front}$, 3 H, NOE to Ar-CH_3 at 1.53, strong NOE to NMe on $C8_{back}$ at 2.90, very weak NOE to 7-H), 1.53 (s, Ar-CH_3 group, NOE to 6.25 and 6.07), 1.22 (d, *J* = 6.7 Hz, 3 H, *i*Pr CH_3 group, NOE to 2.78), 1.18 (d, *J* = 6.9 Hz, 3 H, *i*Pr CH_3 group, NOE to 2.78). ESI-MS: *m*/*z* (%) = 669.16 (100%) ([Ru(η^6-*p*-cymene)Cl(**3a**)]$^+$ model 669.18). MS/MS (669): *m*/*z* (%) = 669.97 ([Ru(η^6-*p*-cymene)Cl(**3a**)]$^+$), 536.52 ([RuCl(**3a**)]$^+$ model 535.07), 482.36, 197.70 ([**1a**-CH_3]$^+$, model $C_{13}H_{13}N_2$ 197.11).

Reaction Between [Ru(*p*-cymene)Cl_2]$_2$ and Protonated Ligand 3a·HBF_4: The reaction was repeated by stirring at room temperature in MeCN with the protonated ligand **3a**·HBF_4 overnight. The only new ^{31}P signal detected was due to the intermediate (postulated to be the dimer) not the final product monomer. ^{31}P NMR (121 MHz, CD_3CN): δ_P = –18.32 (s, **3a**·HBF_4, integral 35), 31.97 (s, integral 1) ppm.

Crystalline *trans*-$PdCl_2$(3a)$_2$ (Orange) with Crystalline Pd_2Cl_4(3a)$_2$ (Yellow): A yellow solution of **3a** (100 mg, 0.25 mmol) in dry ether (0.5 mL) was layered onto a solution of [Pd(COD)Cl_2] (20 mg, 0.07 mmol) in dry CH_2Cl_2 (0.5 mL) in a narrow glass tube. Orange crystals of *trans*-[$PdCl_2$(**3a**)$_2$] and a small quantity of yellow crystals of [Pd_2Cl_4(**3a**)$_2$] slowly formed at the interface. The orange crystals proved to be highly insoluble in most solvents and only sparingly soluble in CH_2Cl_2. Yellow crystals of [Pd_2Cl_4(**3a**)$_2$] were completely soluble in CH_2Cl_2. M.p. ([$PdCl_2$(**3a**)$_2$]) 178–186 °C (decomp.), m.p. ([Pd_2Cl_4(**3a**)$_2$]): 198 °C (decomp.). $PdCl_2$(**3a**)$_2$·CH_2Cl_2: $C_{53}H_{56}Cl_4N_4P_2Pd$: calcd. C 60.22, H 5.34, N 5.30, P 5.87; found C 59.95, H 5.39, N 5.14, P 5.64. ^{31}P NMR ($CDCl_3$, 202 MHz): δ_P = 42.80 {s, [Pd_2Cl_4(**3a**)$_2$]}, trace 32.82 (s, *trans*-[$PdCl_2$(**3a**)$_2$]) ppm. ^1H NMR ($CDCl_3$, 500 MHz): δ_H = 7.81 (ddd, J_{HP} = 13.1, J_{HH} = 8.3, 1.0 Hz, 4 H, 12-H), 7.75 (dd, *J* = 7.7, 1.5 Hz, 1 H, 5-H or 7-H) 7.71 (dd, *J* = 8.5, 1.6 Hz, 1 H, 4-H), 7.67 (dd, *J* = 7.5, 1.5 Hz, 1 H, 5-H or 7-H), 7.62 (dd, *J* = 7.7 Hz, 1 H, 6-H), 7.57 (t, 2 H, 14-H), 7.47 (td, J_{HH} = 8.8, J_{HP} = 3 Hz, 4 H, 13-H), 7.07 (dd, J_{HP} = 9.4, J_{HH} = 8.5 Hz, 1 H, 3-H), 4.19 (s, 6 H, NMe_2), 2.62 (s, 6 H, NMe_2) ppm. *Major impurity*: 6.28 (m, cod, 2.5 H), 5.56 (m, cod, 2 H), 2.35 (m, cod, 4 H) ppm. ESI-MS (CH_2Cl_2/formic acid) selected peaks: *m*/*z* (%) = 974.89 (0.2%, [$PdCl_2$(**3a**)$_2$ + H]$^+$, model 975.23), 581.88 (0.35%, [MeCN·PdCl(**3a**)]$^+$, model 582.08), 485.95 (0.08%, [$PdCl_2$(**3a**)$_2$ – 2H]$^{2+}$, model 486.94). MS/MS (974): *m*/*z* (%) = 974.91 ([$PdCl_2$(**3a**)$_2$ + H]$^+$), 399.09 [**3a** +H]$^+$. ESI-MS (yellow crystals) (MeOH/DCM) selected peaks: *m*/*z* (%) = 1114.84 (100%, [Pd_2Cl_3(**3a**)$_2$]$^+$, model 1115.10), 1078.89 (2%, [Pd_2Cl_2(**3a**) – H]$^+$, model 1079.12), 538.94 (100%, [PdCl·**3a**]$^+$, model 539.07).

Synthesis Using 3a·HBr: ESI-MS (orange product): *m*/*z* (%) = 376.10 (1%, ["Pd"]$^{2+}$), 397.19 [5%, (**3a** – H)]$^+$, 399.20 [1%, (**3a** + H)]$^+$, 486.11 (3%, [$PdCl_2$(**3a** – H)$_2$]$^{2+}$, model $C_{52}H_{52}Cl_2N_4P_2Pd$, 486.61), 575.03 (4%, [$PdCl_2$(**3a** – H)]$^+$, model $C_{26}H_{26}Cl_2N_2PPd$, 575.03), 607.05 (2%), [$PdCl_2$(**3a**) + 31]$^+$, 774.12 (0.5%, [Pd_2Cl_4(**3a** – H)$_2$(**3a**)]$^{2+}$, model $C_{78}H_{79}Cl_4N_6P_3Pd_2$, 774.62), 791.10 (0.2% ["Pd"]$^{2+}$), 827.05 (0.2% ["Pd_2"]$^{2+}$), 844.05 (0.3%, ["Pd_2"]$^{2+}$), 863.03 (0.3%, ["Pd_2"]$^{2+}$), 880.00 (3%, [Pd_3Cl_7(**3a** – H)$_3$]$^{2+}$, model 880.52), 933.45 (0.1%, ["Pd_2"]$^{2+}$).

Synthesis of $PtCl_2$(3a)$_2$: A solution of **3a** (43 mg, 0.11 mmol) in diethyl ether (1.1 mL) was added to a stirring solution of $PtCl_2$(cod) (20 mg, 0.054 mmol) in CH_2Cl_2 (0.7 mL). The pale yellow solution intensified in color on stirring for 6 h after which time stirring of the solution was stopped and ether was carefully layered onto the solution which was left overnight. Microcrystalline yellow $PtCl_2$(**3a**)$_2$ was recovered in two successive crops by filtration and washing with ether: yield 23 mg, 41%, m.p. 236–240 °C (decomp). ^{31}P NMR (400 MHz, $CDCl_3$): δ_P = 15.6 ($^1J_{PPt}$ = 3900 Hz) ppm. ^1H NMR (400 MHz, $CDCl_3$): δ_H = 7.79 (m, 10 H, 8 12-H plus 2 4-H), 7.71 (d, *J* = 2, 8 Hz, 2 H, 5-H or 7-H), 7.69 (d, *J* = 8, 2 Hz, 2 H, 5-H or 7-H), 7.62 (t, *J* = 7.6 Hz, 2 H, 2 6-H), 7.54 (m, 4 H, 4 14-H), 7.45 (t with ^{31}P coupling, 8 13-H), 7.20 (dd, *J* = 8, 9 Hz, 2 H, 3-H), 4.40 [s, 6 H, $N(CH_3)_2$, 1-H or 8-H], 2.62 [s, 6 H, $N(CH_3)_2$, 1-H or 8-H] ppm. ESI-MS (of crude solution, CH_2Cl_2): *m*/*z* (%) = 398.89 (100%, [**3a** + H]$^+$), 1062.58 (15%, [$PtCl_2$(**3a**)$_2$ + H]$^+$) and trace amounts (<1%) of: [PtCl(**3a**)$_2$]$^+$ (1026.65, 0.5%), dimer at 1726.23 (model Pt_2Cl_4(**3a**)$_3$H = 1727.38). MS/MS of [$PtCl_2$(**3a**)$_2$ + H]$^+$ gave exclusively free [**3a** + H]$^+$ at 399.03. MS/MS of the dimer at 1726 gave [$PtCl_2$(**3a**)$_2$ + H]$^+$ and [**3a** + H]$^+$ only.

CCDC-837948 (for **3a**) and CCDC-837947 (for **3b**) contain the supplementary crystallographic data for this paper. These data can be obtained free of charge from The Cambridge Crystallographic Data Centre via www.ccdc.cam.ac.uk/data_request/cif.

Supporting Information (see footnote on the first page of this article): Additional ESI-MS(/MS) and ^1H NMR spectra.

Acknowledgments

N. J. F. thanks Professor Brian F. G. Johnson for support and the Engineering and Physical Sciences Research Council (EPSRC) for a studentship and for current funding (EP/G006792/1), J. S. M. thanks the Natural Sciences and Engineering Research Council (NSERC) of Canada for a Discovery Grant and a Discovery Accelerator Supplement, the Canada Foundation for Innovation (CFI) and the British Columbia Knowledge Development Fund (BCKDF), and the University of Victoria for instrumentation and operational funding. K. V. thanks the University of Victoria for a Pacific Century Fellowship.

[1] K. W. M. Siu, R. Guevremont, J. C. Y. Le Blanc, G. J. Gardner, S. S. Berman, *J. Chromatogr. A* **1991**, *554*, 27–38.
[2] A. J. Canty, P. R. Traill, R. Colton, I. M. Thomas, *Inorg. Chim. Acta* **1993**, *210*, 91–97.
[3] a) M. Bonchio, G. Licini, G. Modena, O. Bortolini, S. Moro, W. A. Nugent, *J. Am. Chem. Soc.* **1999**, *121*, 6258–6268; b) Z. Li, Z. H. Tang, X. X. Hu, C. G. Xia, *Chem. Eur. J.* **2005**, *11*, 1210–1216; c) B. C. Gilbert, J. R. L. Smith, A. Mairata i Payeras, J. Oakes, R. Pons i Prats, *J. Mol. Catal. A* **2004**, *219*, 265–272; d) H. Chen, R. Tagore, G. Olack, J. S. Vrettos, T.-C. Weng, J. Penner-Hahn, R. H. Crabtree, G. W. Brudvig, *Inorg. Chem.* **2007**, *46*, 34–43.
[4] a) P. J. Dyson, K. Russell, T. Welton, *Inorg. Chem. Commun.* **2001**, *4*, 571–573; b) P. Pelagatti, M. Carcelli, F. Calbiani, C. Cassi, L. Elviri, C. Pelizzi, U. Rizzotti, D. Rogolino, *Organometallics* **2005**, *24*, 5836–5844; c) C. Daguenet, R. Scopelliti, P. J. Dyson, *Organometallics* **2004**, *23*, 4849–4857.
[5] C. Vicent, M. Viciano, E. Mas-Marza, M. Sanau, E. Peris, *Organometallics* **2006**, *25*, 3713–3720.
[6] a) S. R. Wilson, Y. Wu, *Organometallics* **1993**, *12*, 1478–1480; b) C. Raminelli, M. H. G. Prechtl, L. S. Santos, M. N. Eberlin, J. V. Comasseto, *Organometallics* **2004**, *23*, 3990–3996; c) C. Chevrin, J. Le Bras, F. Henin, J. Muzart, A. Pla-Quintana, A. Roglans, R. Pleixats, *Organometallics* **2004**, *23*, 4796–4799.
[7] a) J. Masllorens, I. Gonzalez, A. Roglans, *Eur. J. Org. Chem.* **2007**, 158–166; b) A. A. Sabino, A. H. L. Machado, C. R. D. Correia, M. N. Eberlin, *Angew. Chem.* **2004**, *116*, 2568; *Angew. Chem. Int. Ed.* **2004**, *43*, 2514–2518; c) P. A. Enquist, P. Nilsson, P. Sjoberg, M. Larhed, *J. Org. Chem.* **2006**, *71*, 8779–8786; d) A. Svennebring, P. J. R. Sjoberg, M. Larhed, P. Nilsson, *Tetrahedron* **2008**, *64*, 1808–1812; e) C. Chevrin, J. Le Bras, A. Roglans, D. Harakat, J. Muzart, *New J. Chem.* **2007**, *31*, 121–126; f) C. Markert, M. Neuburger, K. Kulicke, M. Meuwly, A. Pfaltz, *Angew. Chem.* **2007**, *119*, 5996; *Angew. Chem. Int. Ed.* **2007**, *46*, 5892–5895.
[8] L. S. Santos (Ed.), *Reactive Intermediates: MS Investigations in Solution*, Wiley-VCH, Weinheim, Germany, **2010**.
[9] A. O. Aliprantis, J. W. Canary, *J. Am. Chem. Soc.* **1994**, *116*, 6985–6986.
[10] a) R. Colton, J. C. Traeger, *Inorg. Chim. Acta* **1992**, *201*, 153–155; b) I. Ahmed, A. M. Bond, R. Colton, M. Jurcevic, J. C. Traeger, J. N. Walter, *J. Organomet. Chem.* **1993**, *447*, 59–65.
[11] a) D. J. F. Bryce, P. J. Dyson, B. K. Nicholson, D. G. Parker, *Polyhedron* **1998**, *17*, 2899–2905; b) C. Decker, W. Henderson, B. K. Nicholson, *J. Chem. Soc., Dalton Trans.* **1999**, 3507–3513.
[12] a) C. Hinderling, C. Adlhart, P. Chen, *Angew. Chem.* **1998**, *110*, 2831; *Angew. Chem. Int. Ed.* **1998**, *37*, 2685–2689; b) C. Adlhart, C. Hinderling, H. Baumann, P. Chen, *J. Am. Chem. Soc.* **2000**, *122*, 8204–8214; c) P. Chen, *Angew. Chem.* **2003**, *115*, 2938; *Angew. Chem. Int. Ed.* **2003**, *42*, 2832–2847.
[13] S. Zhou, B. S. Prebyl, K. D. Cook, *Anal. Chem.* **2002**, *74*, 4885–4888.
[14] N. J. Farrer, R. McDonald, J. S. McIndoe, *Dalton Trans.* **2006**, 4570–4579.
[15] R. W. Alder, *Chem. Rev.* **1989**, *89*, 1215–1223.
[16] a) K. Nagasawa, *Related Organocatalysts (1): A Proton Sponge*, in: *Superbases for Organic Synthesis: Guanidines, Amidines, Phosphazenes and Related Organocatalysts* (Ed.: T. Ishikawa), Wiley, Chichester, U.K., **2007**, pp. 931–1139.
[17] a) R. Shroff, A. Svatos, *Anal. Chem.* **2009**, *81*, 7954–7959; b) R. Shroff, A. Svatos, *Rapid Commun. Mass Spectrom.* **2009**, *23*, 2380–2382.
[18] a) H. A. Staab, T. Saupe, *Angew. Chem.* **1988**, *100*, 895–909; b) S. T. Howard, *J. Am. Chem. Soc.* **2000**, *122*, 8238–8244.
[19] A. F. Pozharskii, A. V. Degtyarev, O. V. Ryabtsova, V. A. Ozeryanskii, M. E. Kletskii, Z. A. Starikova, L. Sobczyk, A. Filarowski, *J. Org. Chem.* **2007**, *72*, 3006–3019.
[20] A. L. Llamas-Saiz, C. Foces-Foces, J. Elguero, *J. Mol. Struct.* **1994**, *328*, 297–323.
[21] R. W. Alder, P. S. Bowman, W. R. S. Steele, D. R. Winterman, *Chem. Commun. (London)* **1968**, 723–724.
[22] H. M. Gilow, D. E. Burton, *J. Org. Chem.* **1981**, *46*, 2221–2225.
[23] a) F. Hibbert, J. Emsley, *Adv. Phys. Org. Chem.* **1990**, *26*, 255–279; b) J. P. H. Charmant, G. C. Lloyd-Jones, T. M. Peakman, R. L. Woodward, *Eur. J. Org. Chem.* **1999**, 2501–2510; c) J. Berthelot, C. Guette, M. Essayegh, P. L. Desbene, J. J. Basselier, *Synth. Commun.* **1986**, *16*, 1641–1645; d) N. V. Vistorobskii, A. F. Pozharskii, *Zh. Org. Khim.* **1989**, *25*, 2154–2161.
[24] C. A. Tolman, *Chem. Rev.* **1977**, *77*, 313–348; O. V. Ryabtsova, A. F. Pozharskii, V. A. Ozeryanskii, N. V. Vistorobskii, *Russ. Chem. Bull.* **2001**, *50*, 854–859.
[25] T. E. Müller, D. M. P. Mingos, *Trans. Met. Chem.* **1995**, *20*, 533–539.
[26] W. Henderson, C. Evans, *Inorg. Chim. Acta* **1999**, *294*, 183–192.
[27] A. D. Phillips, L. Gonsalvi, A. Romerosa, F. Vizza, M. Peruzzini, *Coord. Chem. Rev.* **2004**, *248*, 955–993.
[28] L. S. Santos, G. B. Rosso, R. A. Pilli, M. N. Eberlin, *J. Org. Chem.* **2007**, *72*, 5809–5812.
[29] a) K. L. Vikse, M. A. Henderson, A. G. Oliver, J. S. McIndoe, *Chem. Commun.* **2010**, *46*, 7412–7414; b) K. L. Vikse, Z. Ahmadi, C. C. Manning, D. A. Harrington, J. S. McIndoe, *Angew. Chem. Int. Ed.* **2011**, *50*, 8304–8306.
[30] a) D. M. Chisholm, A. G. Oliver, J. S. McIndoe, *Dalton Trans.* **2010**, *39*, 364–373 ; b) S. L. Jackson, D. M. Chisholm, J. S. McIndoe, L. Rosenberg, *Eur. J. Inorg. Chem.* **2010**, 327–330.
[31] D. M. Chisholm, J. S. McIndoe, *Dalton Trans.* **2008**, 3933–3945.
[32] C. S. Allardyce, P. J. Dyson, D. J. Ellis, S. L. Heath, *Chem. Commun.* **2001**, 1396–1397.

Received: August 2, 2011
Published Online: December 21, 2011

